Monte Carlo Simulation of Error Propagation in the Determination of Binding Constants from Rectangular Hyperbolae. 2. Effect of the Maximum-Response Range

Michael T. Bowser and David D. Y. Chen*

Department of Chemistry, University of British Columbia, 2036 Main Mall, Vancouver, BC, Canada V6T 1Z1

Received: July 8, 1998

Many processes dictated by chemical equilibria can be described by rectangular hyperbolae. Fitting chemical responses to rectangular hyperbolae also allows the binding constants for these equilibria to be estimated. Unfortunately, the propagation of error through the different methods of estimating the binding constants is not well understood. Monte Carlo simulations are used to assess the accuracy and precision of binding constants estimated using a nonlinear regression method and three linear plotting methods. The effect of the difference between the physical response of the uncomplexed substrate and the response of the substrate−ligand complex (i.e., the maximum-response range) was demonstrated using errors typical for a capillary electrophoresis system. It was shown that binding constant estimates obtained using nonlinear regression were more accurate and more precise than estimates from when the other regression methods were used, especially when the maximum-response range was small. The precision of the nonlinear regression method correlated well with the curvature of the binding isotherm. To obtain a precise estimate for the binding constant, the maximum-response range needed to be much larger (over 70 times larger for the conditions used in this experiment) than the error present in individual data points.

Introduction

Rectangular hyperbolae have been used to describe many physicochemical properties influenced by chemical equilibria[1] including UV−vis absorption,[2−7] NMR chemical shifts,[8−13] Michaelis−Menten kinetics,[14−21] ion transport across membranes,[22] pharmacokinetics,[23−26] and even algal growth rates.[27−29] These studies are based on a certain physical response dictated by a 1:1 interaction between a substrate and a ligand. Equations, all taking the form of rectangular hyperbolae, have been developed independently in various research areas such as spectrophotometry, NMR, and Michaelis−Menten kinetics to describe the effect of the equilibrium (see Table 1).[1] In all cases, the physical response is determined by two constants: the equilibrium constant (either expressed as a binding or dissociation constant) and the maximum-response range (representing the difference between the response at zero and infinite ligand concentrations).

Recently, it has been shown that in capillary electrophoresis (CE) analyte mobility in the presence of analyte−additive interactions can be described according to[30−40]

$$(\nu\mu_{ep}^{A} - \mu_{ep,A}) = \frac{(\mu_{ep,AC} - \mu_{ep,A})K_{AC}[C]}{1 + K_{AC}[C]} \qquad (1)$$

where μ_{ep}^{A} is the net electrophoretic mobility of the analyte, ν is a correction factor which normalizes μ_{ep}^{A} to conditions where [C] approaches zero, [C] is the concentration of the complexation additive (analogous to [L]), K_{AC} is the formation constant of the complex AC, and $\mu_{ep,AC}$ and $\mu_{ep,A}$ are the electrophoretic mobilities of the analyte−additive complex AC and the uncomplexed analyte A, respectively. Clearly, eq 1 is analogous to the other equations listed in Table 1.

* To whom correspondence should be addressed. Tel: (604)822-0878. Fax: (604)822-2847. E-mail: chen@chem.ubc.ca.

The equilibrium constants and maximum-response ranges for the equations listed in Table 1 are usually estimated by measuring the response over a range of ligand concentrations followed by one of several regression procedures. Although a nonlinear regression can be used to solve the constants directly, eq 1 is often linearized, allowing the constants to be estimated from the slopes and intercepts of straight lines.[1] The linearized equations have acquired different names in different research fields but can be referred to most generally as double-reciprocal (also referred to as Lineweaver−Burk[15] or Benesi−Hildebrand[2] plots), *y*-reciprocal, and *x*-reciprocal (also referred to as Eadie[16] or Scatchard[41] plots) methods. The linearizations of eq 1 are shown in Table 2.

Although the nonlinear regression and each of the three linearizations are based on the same equation, they often give different estimates and confidence intervals for the constants when applied to the same data set.[42−45] Linearizing the rectangular hyperbola invalidates some of the assumptions made in performing the least-squares regression analysis, including introducing error into the independent variable and transforming the error in the data to a non-Gaussian distribution.[1] The data spacing is also changed, which alters the weight on certain measurements. These problems can often be overcome if the data are weighted according to the functions listed in Table 2.[1]

Because of the complexity of the regression calculations, it is difficult to show how error is propagated through the different methods analytically. Dowd and Riggs[43] first used Monte Carlo analyses to compare the different calculation methods and their estimates of the constants. Since then, a number of researchers have used Monte Carlo analyses to simulate binding experiments.[46−53] It has been shown that the nonlinear regression method minimizes both the error and the bias in the estimates of the constants. Unfortunately, the effect of experimental parameters on the reliability of the estimated binding constants has not been studied thoroughly. We have recently demonstrated

10.1021/jp982917e CCC: $18.00
Published on Web 12/11/1998

TABLE 1: Equations and Maximum-Response Ranges for Absorbance, NMR, Michaelis−Menten Kinetics and Capillary Electrophoresis

technique	equation	maximum-response range
absorbance	$\frac{(A - A_S)}{b} = \frac{[S_0](\epsilon_{SL} - \epsilon_S)K[L]}{1 + K[L]}$	$b[S_0](\epsilon_{SL} - \epsilon_S)$
NMR	$(\delta - \delta_S) = \frac{(\delta_{SL} - \delta_S)K[L]}{1 + K[L]}$	$(\delta_{SL} - \delta_S)$
Michaelis−Menten kinetics	$v = \frac{V_m[S]}{K_m + [S]}$	V_m
capillary electrophoresis	$(\nu\mu_{eq}^A - \mu_{ep,A}) = \frac{(\mu_{ep,AC} - \mu_{ep,A})K_{AC}[C]}{1 + K_{AC}[C]}$	$(\mu_{ep,AC} - \mu_{ep,A})$

TABLE 2: Equations Used in Capillary Electrophoresis and Variances in the Transformed *y* for the Different Calculation Methods

calculation method	equation	σ_y^2 [a]
nonlinear regression	$(\nu\mu_{ep}^A - \mu_{ep,A}) = \frac{(\mu_{ep,AC} - \mu_{ep,A})K_{AC}[C]}{1 + K_{AC}[C]}$	σ_y^2
double-reciprocal	$\frac{1}{(\nu\mu_{ep}^A - \mu_{ep,A})} = \frac{1}{(\mu_{ep,AC} - \mu_{ep,A})K_{AC}}\frac{1}{[C]} + \frac{1}{(\mu_{ep,AC} - \mu_{ep,A})}$	$\frac{\sigma_y^2}{(\nu\mu_{ep}^A - \mu_{ep,A})^4}$
y-reciprocal	$\frac{[C]}{(\nu\mu_{ep}^A - \mu_{ep,A})} = \frac{[C]}{(\mu_{ep,AC} - \mu_{ep,A})} + \frac{1}{(\mu_{ep,AC} - \mu_{ep,A})K_{AC}}$	$\frac{[C]^2\sigma_y^2}{(\nu\mu_{ep}^A - \mu_{ep,A})^4}$
x-reciprocal	$\frac{(\nu\mu_{ep}^A - \mu_{ep,A})}{[C]} = -K_{AC}(\nu\mu_{ep}^A - \mu_{ep,A}) + K_{AC}(\mu_{ep,AC} - \mu_{ep,A})$	$\left(K_{AC} + \frac{1}{[C]}\right)^2 \sigma_y^2$

[a] $\sigma_{y'}^2$ is the variance of the transformed *y*; σ_y^2 is the variance in $(\nu\mu_{ep}^A - \mu_{ep,A})$; the weight for each point is equal to $1/\sigma_{y'}^2$.

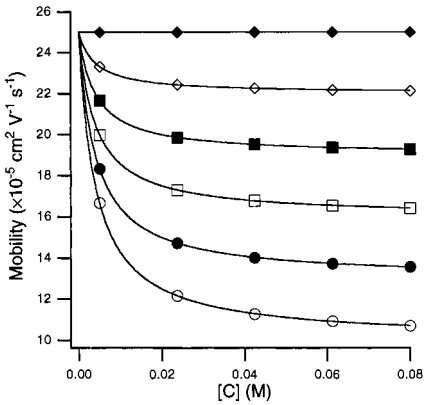

Figure 1. Binding isotherms with different maximum-response ranges. The constants used to draw the curves are $K = 250\ M^{-1}$; $\mu_{ep,A} = 0.000\ 25\ cm^2 \cdot V^{-1} \cdot s^{-1}$; and $\mu_{ep,AC} = 0.000\ 25$ (◆), 0.000 22 (◇), 0.000 19 (■), 0.000 16 (□), 0.000 13 (●), and 0.000 10 $cm^2 \cdot V^{-1} \cdot s^{-1}$ (○).

the effect of the ligand concentration range on the accuracy and precision of binding-constant estimates using Monte Carlo analyses.[54]

Another concern is the effect of the maximum-response range on the reliability of the binding-constant estimate. As shown in Figure 1, if the maximum-response range is zero, the binding isotherm takes the shape of a straight line, making it impossible to estimate the binding constant. The specific constants that determine the maximum-response range in UV−vis absorption, NMR, Michaelis−Menten kinetics, and CE are listed in Table 1.

In this paper, the effect of the maximum-response range on the accuracy and precision estimated binding constants is studied. Nonlinear regression is compared with the three linearizations of the binding isotherm. Terminology developed for CE (eq 2) will be used because this is the primary research interest of our group (i.e., analyte and additive are analogous to substrate and ligand, respectively). Therefore, the constants and errors in the data are typical for CE. It should be emphasized that although CE is used as an example in this paper the equations are analogous to those used in many other research areas (see Table 1), allowing the conclusions presented here to be applied to complexation chemistry in general.

Methods

Monte Carlo simulations of a dynamic-complexation CE experiment were performed using a Visual Basic macro in Microsoft Excel 5.0 on a Pentium PC. The simulations were made assuming the following: $\mu_{ep,A} = -2.5 \times 10^{-4}\ cm^2 \cdot V^{-1} \cdot s^{-1}$; $K = 250\ M^{-1}$; separation potential = −30 kV; total capillary length = 57 cm; length to the detector = 50 cm. The additive concentrations used to perform the simulations were 5, 23.75, 42.5, 61.25, and 80 mM which were shown in an earlier paper to approximately cover the optimum concentration range for $K = 250\ M^{-1}$.[54] Simulations were made for $\mu_{ep,AC}$ ranging from -1×10^{-4} to $-2.5 \times 10^{-4}\ cm^2 \cdot V^{-1} \cdot s^{-1}$. Equation 1 was used to calculate the true net analyte mobility at each additive concentration. The random number generator in Excel 5.0 was used to produce an experimental mobility according to a normal distribution which had a mean equal to the true mobility and a standard deviation of $8.75 \times 10^{-7}\ cm^2 \cdot V^{-1} \cdot s^{-1}$. Two experimental mobilities were generated for each additive concentration. Four experimental mobilities were generated for an additive

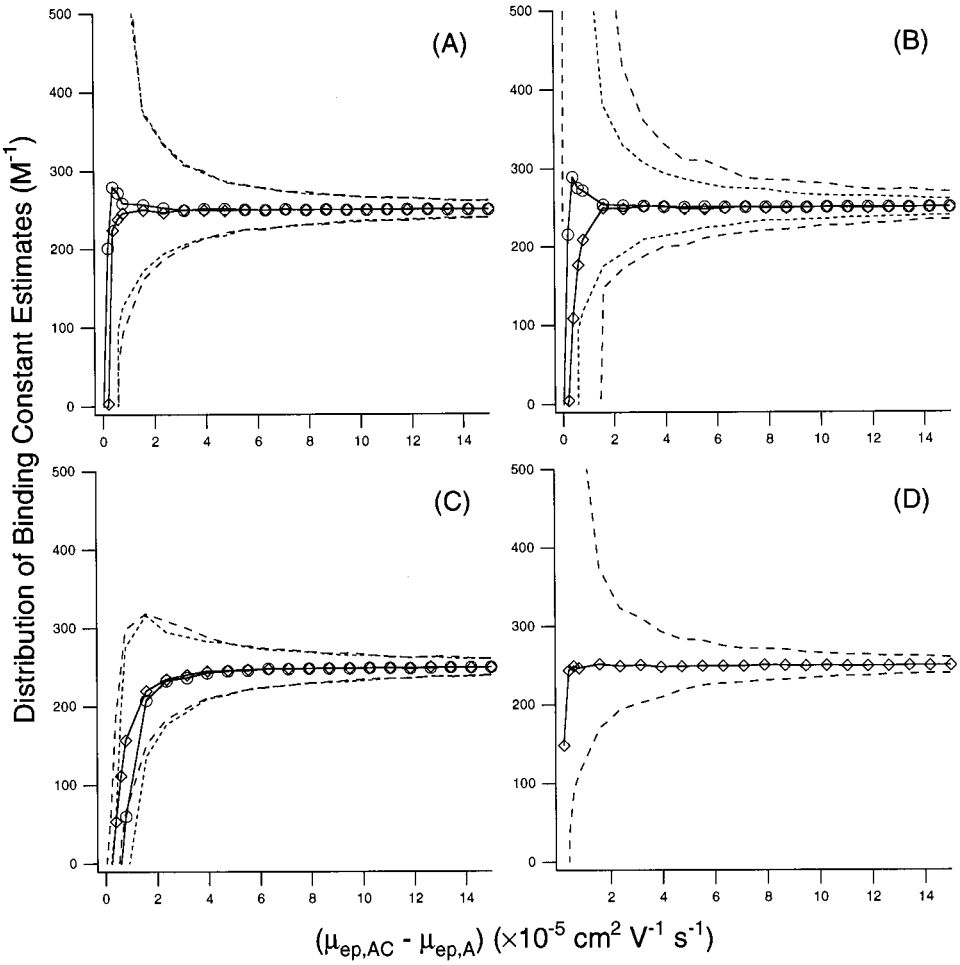

Figure 2. Distributions of the binding constants estimated using the (A) double-reciprocal, (B) *y*-reciprocal, (C) *x*-reciprocal, and (D) nonlinear regression methods for $(\mu_{ep,AC} - \mu_{ep,A}) = 0$ to 15×10^{-5} $cm^2 \cdot V^{-1} \cdot s^{-1}$. The markers ◇ and ○ represent the medians of the unweighted and weighted methods, respectively. The dashed lines define the 95% ranges for the unweighted (− −) and weighted (- - -) methods.

concentration of 0 mM, again with a standard deviation of 8.75 $\times$ 10^{-7} $cm^2 \cdot V^{-1} \cdot s^{-1}$, to calculate $\mu_{ep,A}$. The experimental mobilities were then used to estimate the equilibrium constant according to one of the four calculation methods. All regressions were made according to the least-squares variance−covariance method. This procedure was repeated 1000 times for each calculation method at each $\mu_{ep,AC}$. A total of 23 values for $\mu_{ep,AC}$ were tested, giving rise to over 2.25 million simulated measurements, emphasizing the necessity of the computational approach used.

Results and Discussion

Distribution of Binding-Constant Estimates. Figure 2 shows the distributions of the binding constants estimated using the nonlinear regression and the three linear transformations. The markers represent the medians of the distributions. Medians were chosen to represent the central tendency of the distributions because of their robustness and insensitivity to the grossly inaccurate estimates that sometimes occur when experiments are performed under nonideal conditions. The dashed lines bound the range of the distribution that includes 95% of the binding-constant estimates (i.e., the 95% range). Therefore, 2.5% of the binding-constant estimates were above the upper dashed line, and 2.5% of the estimates were below the lower dashed line.

The 95% range of the estimated binding constants gives an indication as to the precision of the method under a certain set of conditions. A narrow range of binding constants indicates that an experiment performed under those conditions is more likely to give an estimate that is close to the actual value of the binding constant. As expected, the range of binding-constant estimates generally increased as the maximum-response range (i.e., $\mu_{ep,AC} - \mu_{ep,A}$) decreased. However, there were some differences in the results obtained from the different calculation methods. The 95% ranges for the *x*-reciprocal plots did not increase as drastically as with the other methods, but the results were significantly biased when the maximum-response range was small. Weighting narrowed the 95% range when the *y*-reciprocal plot was used but had little effect when the double reciprocal or *x*-reciprocal plots were used. Because the error in each data point was equal, there was no difference between the unweighted and weighted nonlinear regression methods. Figure 3 compares the magnitudes of the 95% ranges for the different calculation methods. The ranges for the nonlinear, double-reciprocal, and weighted *y*-reciprocal plots were similar, indicating that the binding constant should be estimated using one of these methods. The unweighted *y*-reciprocal plots gave the widest 95% ranges. Narrow 95% ranges were achieved using *x*-reciprocal plots, but bias makes it an unsuitable method for estimating the binding constant when the maximum-response range is small.

Comparing the medians of the distributions to the true value of the binding constant ($K = 250$ M^{-1} in this case) demonstrates the accuracy of the different calculation methods. As shown in Figure 4, bias did become significant as the maximum-response

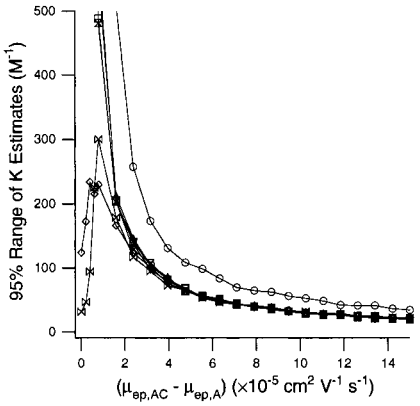

Figure 3. 95% ranges of binding constants estimated using the double-reciprocal (△), weighted double-reciprocal (□), *y*-reciprocal (○), weighted *y*-reciprocal (▽), *x*-reciprocal (◇), weighted *x*-reciprocal (⋈), and nonlinear regression methods (⊠) for ($\mu_{ep,AC} - \mu_{ep,A}$) = 0 to 15 × 10^{-5} cm^2·V^{-1}·s^{-1}.

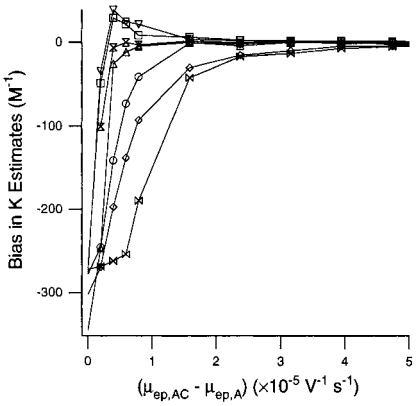

Figure 4. Bias in the distribution of binding constants estimated using the double-reciprocal (△), weighted double-reciprocal (□), *y*-reciprocal (○), weighted *y*-reciprocal (▽), *x*-reciprocal (◇), weighted *x*-reciprocal (⋈), and nonlinear regression methods (⊠) for ($\mu_{ep,AC} - \mu_{ep,A}$) = 0 to 5 × 10^{-5} cm^2·V^{-1}·s^{-1}.

range decreased, especially when data were plotted using *x*-reciprocal plots. Bias is troublesome because it cannot be eliminated through replicate measurements. Although the precision of the constants estimated using *x*-reciprocal plots was good, the accuracy was not. In this simulation, *x*-reciprocal plots consistently gave the wrong value for *K* when the maximum-response range was small. Bias was also present in the double-reciprocal and *y*-reciprocal plots when $\mu_{ep,AC}$ approached $\mu_{ep,A}$. When the maximum-response range was small, weighting in the double-reciprocal and *y*-reciprocal plots overcompensated the error, giving rise to a slightly positive bias. Overall, bias was least significant when the nonlinear regression method was used. The combination of higher accuracy and higher precision makes the nonlinear regression the most reliable method for estimating the binding constant, especially when the maximum-response range is low. This corresponds well with a previous paper, which demonstrated that the nonlinear regression method makes more reliable binding-constant estimates when the additive concentrations are above or below the optimum range.[54] Because of the general availability of personal computers, there does not seem to be any compelling reason to continue using the linear transformations to estimate binding constants. Although the linear transformations should not be used to estimate the binding constant, they are still useful in determining if a 1:1 equilibrium model accurately describes the data.[1,55]

Semiempirical Prediction of the 95% Range. In an earlier paper, we were able to show that the effect of the additive concentration range on the precision of the binding-constant estimates (i.e., the 95% range) could be explained by the amount of curvature in the binding isotherm.[54] The difference in the slope of the curve at the lowest and highest additive concentrations gives a measure of the amount of curvature present in the isotherm. The slope at any point on the isotherm is equal to the derivative of eq 1 with respect to [C]:

$$\frac{\partial(\nu\mu_{ep}^{A})}{\partial[C]} = \frac{(\mu_{ep,AC} - \mu_{ep,A})K_{AC}}{(1 + K_{AC}[C])^2} \quad (2)$$

Clearly, the slope is influenced by the maximum-response range as well as the binding constant and the additive concentration. As shown in Figure 1, the amount of curvature in the binding isotherm decreases as the maximum-response range decreases. When the fraction of analyte complexed is high, the slope of the isotherm approaches zero. When the fraction of analyte complexed is low, the slope of the isotherm approaches

$$\frac{\partial(\nu\mu_{ep}^{A})}{\partial[C]} = (\mu_{ep,AC} - \mu_{ep,A})K_{AC} \quad (3)$$

Therefore, when data are collected over a large portion of the isotherm, the difference in slope between the lowest and highest additive concentrations is approximately

$$\Delta\text{slope} \approx (\mu_{ep,AC} - \mu_{ep,A})K_{AC} \quad (4)$$

The difference in slope is almost linearly related to the maximum-response range if data are collected over a substantial portion of the binding isotherm.

Figure 5A shows the correlation between the reciprocal of the difference in the slope and the relative 95% range of the binding-constant estimates. The correlation is excellent up to a relative 95% range of 1 (i.e., the 95% range is equal to 250 M^{-1} in this case). Above 1, the relative 95% ranges begin to increase faster than the reciprocal of the difference in the slope. Figure 5B compares the curve predicted from the correlation in Figure 5A to the 95% ranges generated by the simulations. The curve corresponds well to the data, indicating that the difference between the slopes at the lowest and highest additive concentrations accurately describes the effect of the maximum-response range on the precision of the binding-constant estimate.

The magnitude of the maximum-response range necessary to make a precise estimate of the binding constant was much higher than expected. As can be seen in Figure 5B, for 95% of the binding-constant estimates to be within 10% of the true value of the binding constant (i.e., 95% range = 50 M^{-1} in this case), ($\mu_{ep,AC} - \mu_{ep,A}$) must be 6.3 × 10^{-5} cm^2·V^{-1}·s^{-1} or higher. This is 72 times the standard deviation of the individual data points. Although the size of the maximum-response range required to achieve a certain level of precision will depend on other factors as well (e.g., number of data points, range of additive concentrations, data spacing, etc.), it is clear that the maximum-response range must be significantly larger than the error in the data points.

In binding experiments, the errors in the individual data points and the maximum-response range are linked, similar to the way that the equilibrium constant is linked to the ligand concentration range.[54] To make a reliable estimate of the binding constant, the maximum-response range must be maximized, but this cannot be done at the expense of the error in the data. Therefore, experiments must be designed to both maximize the response range and minimize the error in the data. An examination of

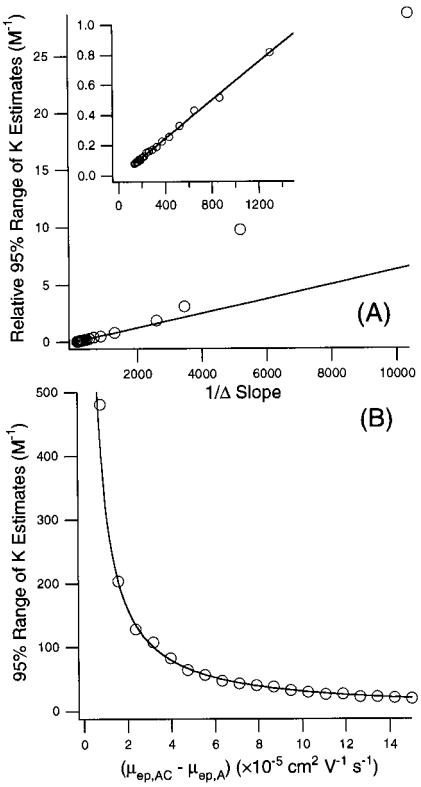

Figure 5. (A) Correlation between the relative 95% ranges of binding constants estimated using the nonlinear regression method and the inverse of the difference between the slopes at the lowest and highest additive concentrations. (B) Comparison between the 95% ranges of binding constants estimated using the nonlinear regression method and the curve predicted using the correlation shown in part A.

the maximum-response ranges listed in Table 1 gives some suggestions as to how this can be done. In UV−vis absorbance, the maximum-response range can be increased by increasing the optical path length or the concentration of the substrate. In NMR studies, the maximum-response range cannot be adjusted because the chemical shifts are intrinsic properties of the substrate and the substrate−ligand complex. However, the error in the chemical responses decreases as the field strength of the instrument is increased, allowing a more precise estimate of the binding constant. Methods for increasing the maximum-response range in Michaelis−Menten kinetics and CE are less clear. Because data are collected as reaction times or migration times, perhaps emphasis should be placed on reducing the error in the time measurements.

Conclusions

It was shown that the nonlinear regression method obtained the most accurate and precise estimates for the binding constant as the maximum-response range was decreased. This, combined with the evidence that the nonlinear regression method is superior to the linear transformations when data are collected outside the ideal additive concentration range,[54] strongly suggests that the nonlinear regression method should be used when estimating binding constants.

It was also shown that the difference in the slope of the binding isotherm at the lowest and highest additive concentrations is a good indicator of the precision of a binding constant estimated using a certain set of conditions. To make a good estimate of the binding constant, the maximum-response range must be significantly higher than the error in the individual data points.

Acknowledgment. This work was supported by the Natural Sciences and Engineering Research Council (NSERC) of Canada. M.T.B. acknowledges a postgraduate scholarship from NSERC.

References and Notes

(1) Connors, K. A. *Binding Constants: The Measurement of Molecular Complex Stability*; John Wiley & Sons: Toronto, 1987.

(2) Benesi, H.; Hildebrand, J. H. *J. Am. Chem. Soc.* **1949**, *71*, 2703−7.

(3) Ramette, R. W. *J. Chem. Educ.* **1967**, *44*, 647−54.

(4) McBryde, W. A. E. *Talanta* **1974**, *21*, 979−1004.

(5) Slama-Schwok, A.; Teulade-Fichou, M. P.; Vigneron, J. P.; Taillandier, E.; Lehn, J. M. *J. Am. Chem. Soc.* **1995**, *117*, 6822−30.

(6) Lahiri, J.; Fate, G. D.; Ungashe, S. B.; Groves, J. T. *J. Am. Chem. Soc.* **1996**, *118*, 2347−58.

(7) Grabner, G.; Monti, S.; Marconi, G.; Mayer, B.; Klein, C.; Köhler, G. *J. Phys. Chem.* **1996**, *100*, 20068−75.

(8) Mathur, R.; Becker, E. D.; Bradley, R. B.; Li, N. C. *J. Phys. Chem.* **1963**, *67*, 2190−4.

(9) Hanna, M. W.; Ashbaugh, A. L. *J. Phys. Chem.* **1964**, *68*, 811−6.

(10) Carper, W. B.; Buess, C. M.; Hipp, G. R. *J. Phys. Chem.* **1970**, *74*, 4229−34.

(11) Seal, B. K.; Mukherjee, A. K.; Mukherjee, D. C.; Farrel, P. G.; Westwood, J. V. *J. Magn. Reson.* **1983**, *51*, 318−22.

(12) Blixt, J.; Detellier, C. *J. Am. Chem. Soc.* **1995**, *117*, 8536−40.

(13) Godínez, L. A.; Patel, S.; Criss, C. M.; Kaifer, A. E. *J. Phys. Chem.* **1995**, *99*, 17449−55.

(14) Michaelis, L.; Menten, M. L. *Biochem. Z.* **1913**, *49*, 333−69.

(15) Lineweaver, H.; Burk, D. *J. Am. Chem. Soc.* **1934**, *56*, 658−66.

(16) Eadie, G. S. *J. Biol. Chem.* **1942**, *146*, 85−93.

(17) Coolen, H. K. A.; Meeuwis, J. A. M.; van Leeuwen, P. W. N. M.; Nolte, R. J. M. *J. Am. Chem. Soc.* **1995**, *117*, 11906−13.

(18) Sun, S.; Duggleby, R. G.; Schowen, R. L. *J. Am. Chem. Soc.* **1995**, *117*, 7317−22.

(19) Corey, E. J.; Noe, M. C. *J. Am. Chem. Soc.* **1996**, *118*, 319−29.

(20) Lamm, G.; Wong, L.; Pack, G. R. *J. Am. Chem. Soc.* **1996**, *118*, 3325−31.

(21) Guedes da Silva, M. F. C.; Silva, J. A. L.; Fraústo da Silva, J. J. R.; Pombeiro, A. J. L.; Amatore, C.; Verpeaux, J.-N. *J. Am. Chem. Soc.* **1996**, *118*, 7568−73.

(22) Aronson, J. K. *Clin. Sci.* **1990**, *78*, 247−54.

(23) Hoang, K.-C. T. *Toxicol. Lett.* **1995**, *79*, 99−106.

(24) Chen, T.-L.; Kennedy, M. J.; Anderson, L. W.; Kiraly, S. B.; Black, K. C.; Colvin, O. M.; Grochow, L. B. *Drug Metab. Dispos.* **1997**, *25*, 544−51.

(25) Kwon, Y.; Morris, M. E. *Pharm. Res.* **1997**, *14*, 774−9.

(26) Kwon, Y.; Morris, M. E. *Pharm. Res.* **1997**, *14*, 780−5.

(27) MacIsaac, J. J.; Dugdale, R. C. *Deep-Sea Res.* **1969**, *16*, 45−57.

(28) Mullin, M. M.; Stewart, E. F.; Fuglister, F. J. *Limnol. Oceanogr.* **1975**, *20*, 259−62.

(29) Verity, P. G. *Limnol. Oceanogr.* **1991**, *36*, 729−50.

(30) Wren, S. A. C.; Rowe, R. C. *J. Chromatogr.* **1992**, *603*, 235−41.

(31) Wren, S. A. C.; Rowe, R. C. *J. Chromatogr.* **1992**, *609*, 363−7.

(32) Wren, S. A. C. *J. Chromatogr.* **1993**, *636*, 57−62.

(33) Shibukawa, A.; Lloyd, D. K.; Wainer, I. W. *Chromatographia* **1993**, *35*, 419−29.

(34) Penn, S. G.; Goodall, D. M.; Loran, J. S. *J. Chromatogr.* **1993**, *636*, 149−52.

(35) Penn, S. G.; Bergstrom, E. T.; Goodall, D. M.; Loran, J. S. *Anal. Chem.* **1994**, *66*, 2866−73.

(36) Penn, S. G.; Bergstrom, E. T.; Knights, I.; Liu, G.; Ruddick, A.; Goodall, D. M. *J. Phys. Chem.* **1995**, *99*, 3875−80.

(37) Rundlett, K. L.; Armstrong, D. W. *J. Chromatogr.* **1996**, *721*, 173−86.

(38) Bowser, M. T.; Sternberg, E. D.; Chen, D. D. Y. *Electrophoresis* **1997**, *18*, 82−91.

(39) Peng, X.; Bowser, M. T.; Britz-McKibbin, P.; Bebault, G. M.; Morris, J.; Chen, D. D. Y. *Electrophoresis* **1997**, *18*, 706−16.

(40) Peng, X.; Bebault, G. M.; Sacks, S. L.; Chen, D. D. Y. *Can. J. Chem.* **1997**, *75*, 507−17.

(41) Scatchard, G. *Ann. N. Y. Acad. Sci.* **1949**, *51*, 660−72.

(42) Dixon, M. *Nature* **1959**, *184*, 296−8.
(43) Dowd, J. E.; Riggs, D. S. *J. Biol. Chem.* **1965**, *240*, 863−9.
(44) Deranleau, D. A. *J. Am. Chem. Soc.* **1969**, *91*, 4044−9.
(45) Atkins, G. L.; Nimmo, I. A. *Anal. Biochem.* **1980**, *104*, 1−9.
(46) Ritchie, R. J.; Prvan, T. *J. Theor. Biol.* **1996**, *178*, 239−54.
(47) Berges, J. A.; Montagnes, D. J. S.; Hurd, C. L.; Harrison, P. L. *Mar. Ecol.: Prog. Ser.* **1994**, *114*, 175−83.
(48) Sagnella, G. A. *Clin. Sci.* **1994**, *87*, 371−81.
(49) Tseng, S.; Hsu, J.-P. *J. Theor. Biol.* **1990**, *145*, 457−64.
(50) Currie, D. J. *Biometrics* **1982**, *38*, 907−19.
(51) Atkins, G. L.; Nimmo, I. A. *Biochem. J.* **1975**, *149*, 775−7.
(52) Madsen, B. W.; Robertson, J. S. *J. Pharm. Pharmacol.* **1974**, *26*, 807−13.
(53) Cornish-Bowden, A.; Eisenthal, R. *Biochem. J.* **1974**, *139*, 721−30.
(54) Bowser, M. T.; Chen, D. D. Y. *J. Phys. Chem. A* **1998**, *102*, 8063−8071.
(55) Bowser, M. T.; Chen, D. D. Y. *Anal. Chem.* **1998**, *70*, 3261−3270.